Fig. S1: The full *m/z* ratios, 700-1800, of CstR (A-C) and CsoR (D-F). A and D are unreacted controls, B and E were reacted with SeO_3^{2-}, and C and F reacted with TeO_3^{2-} as described in the materials and methods. Unreacted CstR displays a *m/z* range from +6 to +13 and cross-linked CstR ranges from +11 to +20. Unreacted CsoR displays a *m/z* range from +7 to +15 and cross-linked CsoR from +13 to +23.

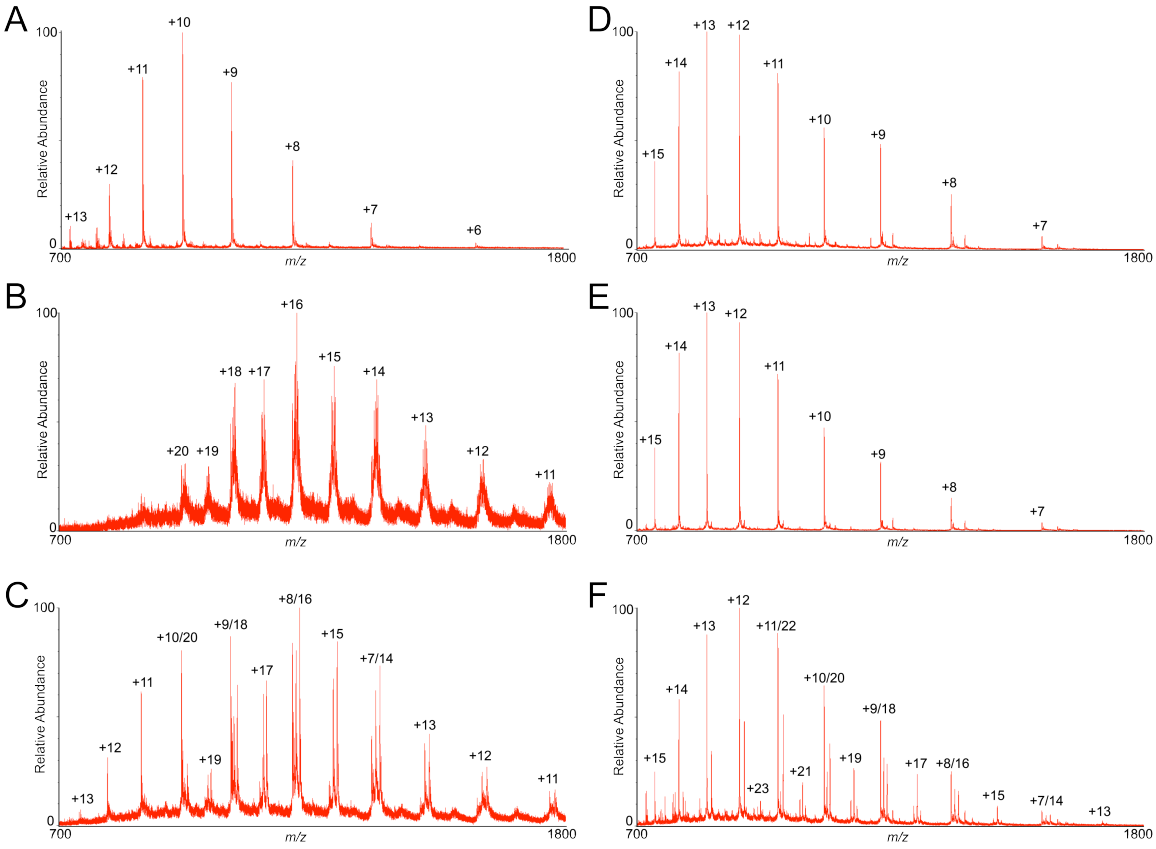

Fig. S2: Fragmentation patterns of the Cys31 (A), MMEEGKDCKDVITQISASK, and Cys60 (B), LMGIIISENLIECVK, containing peptides from a tryptic digest of reduced CstR. Both peptides readily fragment as most ions are readily observed. These spectra were used to help identify cross-linked CstR peptides.

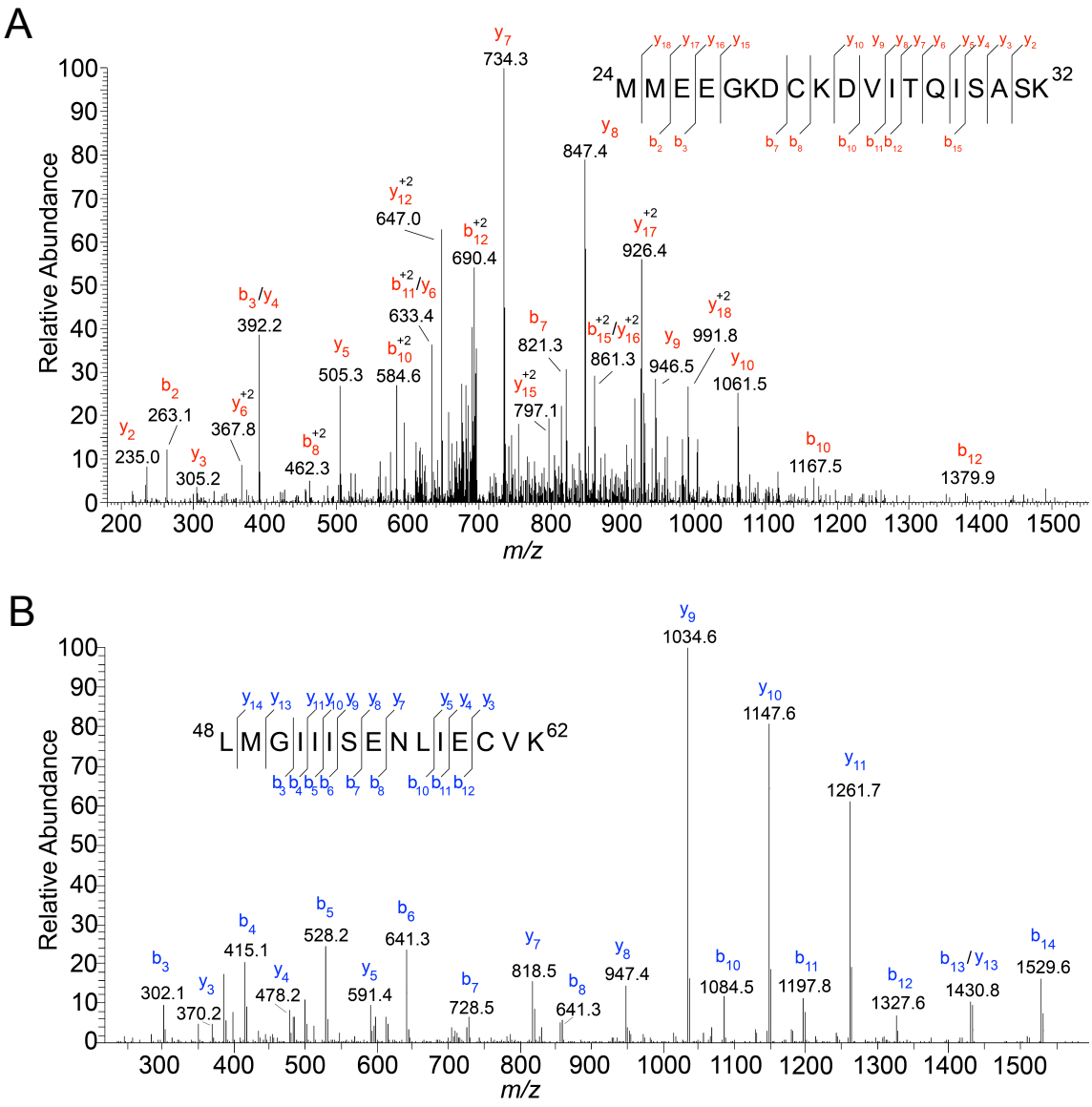

Fig. S3: CstR reacted with SeO_3^{2-} contains prominent disulfide peaks with oxidized cysteine residues. (A) Sum of +4 ions detected over the elution range of CstR cross-linked species. The labeled cross-linked peptides are; **1**, disulfide cross-linked CstR (fragmentation pattern in Fig. 2B, main text); **2**, disulfide cross-linked CstR with one oxidized methionine (fragmentation data not shown); **3**, disulfide cross-linked CstR with two oxygen atoms distributed between the cysteine residues (fragmentation shown in panel B); **4**, Same as **3** with an oxidized methionine (fragmentation data not shown); **5**, selenotrisulfide cross-linked CstR (fragmentation pattern in Fig. 3D, main text); **6**, selenotrisulfide cross-linked CstR with one oxidized methionine (fragmentation data not shown). (B) Fragmentation pattern of disulfide cross-linked CstR with two cysteine oxidations (peak **3** from panel A). Cross-linked AB_{yn} ions contain a mass shift of +32 Da and correspond to two total oxygen atom adductions on one or both cysteine Sγ atom. An oxidation of either Met residue on peptide "A" yields an A_{b7} ion with a mass of approximately 837 or 853 Da for one or two oxygen atoms, respectively. The observed A_{b7} ion has a mass consistent with the reduced state, 821 Da. Similarly, a Met residue oxidation on peptide "B" would yield B_{bn} ions with a mass shift of +16 or +32 Da, *e.g.,* the observed B_{b3} ion would shift to approximately 318 or 334 Da with one or two oxygen atoms, respectively. As a result, we conclude that the oxygen adducts here (*) are assignable as either a mixture of thiosulfonates or α-disulfoxide (Fig. 4, main text).

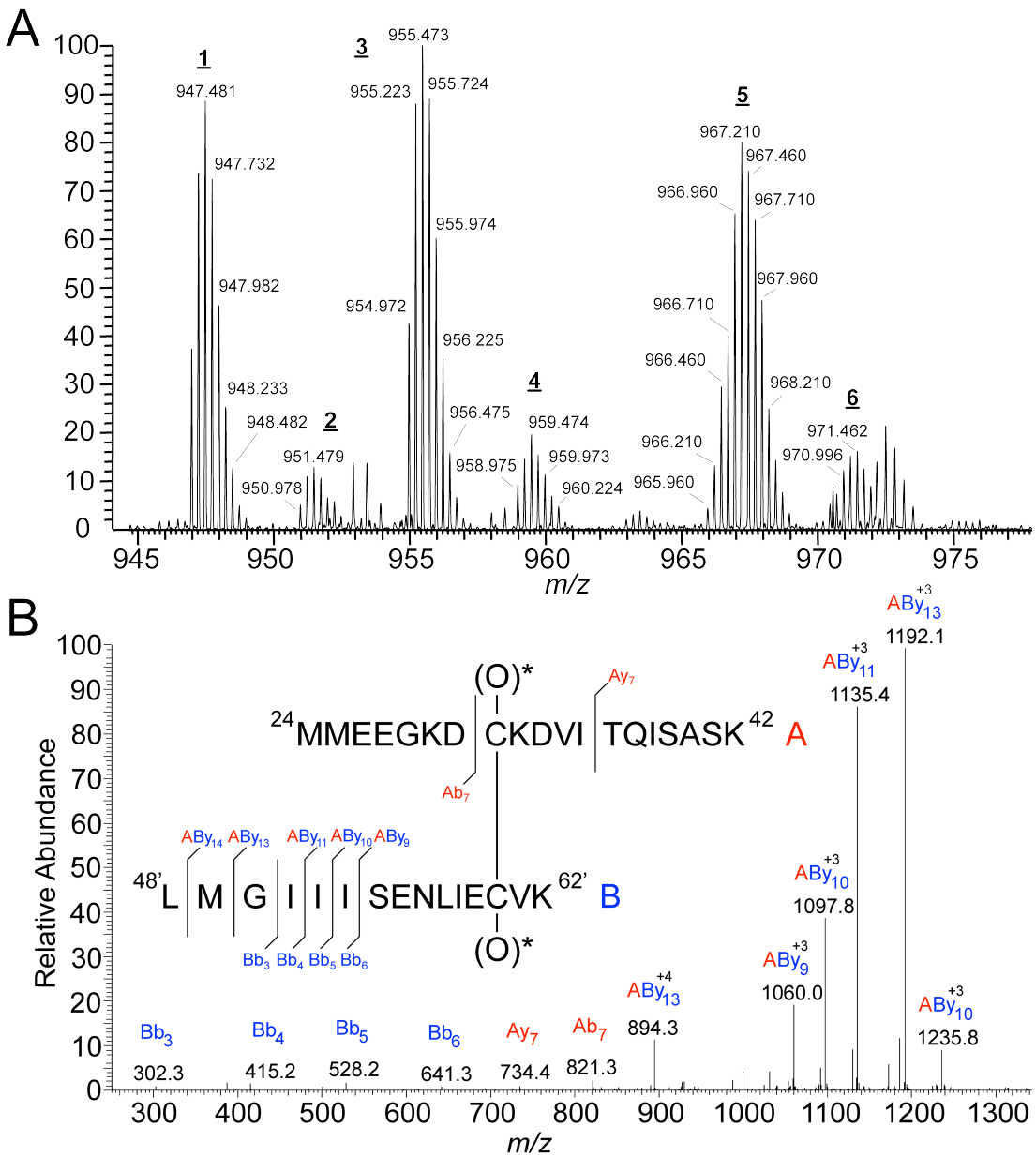

Fig. S4: Reaction products observed by ESI-MS from the reaction (17 h, RT) of C31A CstR (A and B) and C60A CstR (C and D) with tetrathionate (panels A and C) and SeO_3^{2-} (panels B and D). Deconvoluted masses from these spectra are shown in Table S4. Addition of tetrathionate to C31A CstR leads to the formation of disulfide cross-linked CstR as ^{60}CysS-SCys$^{60'}$ likely across the tetramer interface (see Fig. 1, main text) (*m/z* of +12 to +24). The analogous reaction with C60A CstR forms nearly exclusively ^{31}CysS-S_2O_3 (*m/z* of +7 to +12). Reaction with selenite (panels B and D) leads to significant unreacted, reduced CstRs and a mixture of products dominated by the di- and selenotrisulfide cross-linked species, again likely linking cysteines on different dimers. In addition to these species, the reaction of C60A CstR with selenite (panel D) also yields a detectable amount of the monofunctionalized ^{31}CysS-SeO_3^{2-} (*filled* circles) (Table S4). The small amount of this product is consistent with that of a reaction intermediate on pathways to cross-linked species, although this was not investigated here. (E) Fluorescence anisotropy titrations of reduced C31A (open circles*) or C60A (open squares*) CstR before and following full derivatization with selenite (closed symbols). Derivatization was complete after 48 h. *Titrations shown are the same as those shown in Fig. 5, main text.

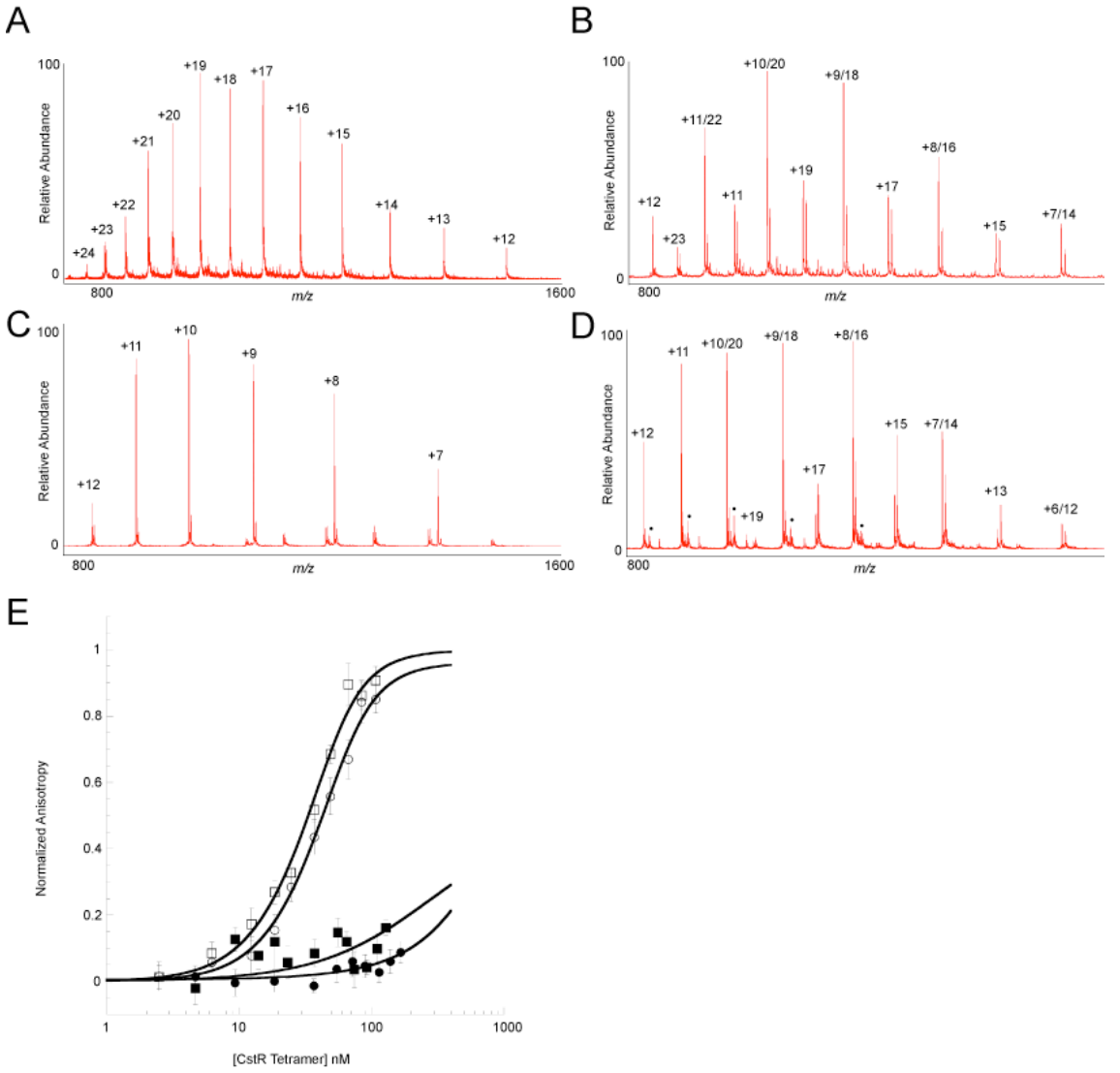

Table S1: CstR cysteine mutant Quikchange™ mutagenesis primers used in this study. Underlined characters are bases changed to introduce cysteine to alanine mutations. *cst* OP1 corresponds to the DNA used in fluorescence anisotropy experiments where 'F' denotes fluorescein.

Primer	Direction	Primer Sequence
C31A CstR	Forward	GGAGGAAGGAAAAGACGCTAAAGATGTCATTAC
	Reverse	GTAATGACATCTTTAGCGTCTTTTCCTTCCTCC
C60A CstR	Forward	GTGAGAATTTAATAGAAGCTGTAAAAGCAGCTGCGG
	Reverse	CCGCAGCTGCTTTTACAGCTTCTATTAAATTCTCAC
cst OP 1	Forward	ATGTGTCAAATACCCCTAGAGGTATTTG
	Reverse	F-CAAATACCTCTAGGGGTATTTGACACAT

Table S2: Summary of deconvoluted CstR masses observed by LC-ESI-MS. All mass shifts are relative to $CstR^{RS\text{-}H}$ or $CstR_2^{(RS\text{-}SR')}$ as indicated by (-).

Modifier	M_r Expected	M_r Observed	Mass Shift	Assignment
None	9641.2	9641.3	-	$CstR^{RS\text{-}H}$
	9663.2	6443.4	22.1	$CstR^{RS\text{-}H}$ + Na
	19280.4	19282.3	-	$CstR_2^{RS\text{-}SR'}$
SeO_3^{2-}	9641.2	9638.2	-	$CstR^{RS\text{-}H}$
	9663.2	9660.4	22.2	$CstR^{RS\text{-}H}$ + Na
	19280.4	19277.5	-	$CstR_2^{RS\text{-}SR'}$
	19312.4	19309.7	32.2	$CstR_2^{RS\text{-}SR'}$ + 2 O
	19359.4	19357.4	79.9	$CstR_2^{RS\text{-}Se\text{-}SR'}$
	19391.4	19389.6	112.1	$CstR_2^{RS\text{-}Se\text{-}SR'}$ + 2 O
	19425.4	19422.5	145	$CstR_2^{RS\text{-}Se\text{-}SR'}$ + 3 Na
	19438.3	19437.1	159.6	$CstR_2^{(RS\text{-}Se\text{-}SR')2}$
	19470.3	19468.8	191.3	$CstR_2^{(RS\text{-}Se\text{-}SR')2}$ + 2 O
	19503.4	19500.3	222.8	$CstR_2^{(RS\text{-}Se\text{-}SR')2}$ + 3 Na
	19517.3	19515.8	238.3	$CstR_2^{(RS\text{-}Se\text{-}SR')2}$ + Se
TeO_3^{2-}	9641.2	9640.2	-	$CstR^{RS\text{-}H}$
	9657.2	9656.2	16	$CstR^{RS\text{-}H}$ + O
	9673.2	9671.6	31.4	$CstR^{RS\text{-}H}$ + 2 O
	9768.8	9767.5	127.3	$CstR^{RS\text{-}H}$ + Te
	19280.4	19279.7	-	$CstR_2^{RS\text{-}SR'}$
	19312.4	19311.4	31.7	$CstR_2^{RS\text{-}SR'}$ + 2 O
	19408	19407.3	127.6	$CstR_2^{RS\text{-}Te\text{-}SR'}$
	19440	19439.1	159.4	$CstR_2^{RS\text{-}Te\text{-}SR'}$ + 2 O
	19535.6	19534.6	254.9	$CstR_2^{(RS\text{-}Te\text{-}SR')2}$
	19567.6	19567.6	287.9	$CstR_2^{(RS\text{-}Te\text{-}SR')2}$ + 2 O
$S_4O_6^{2-}$	9641.2	-	-	$CstR^{RS\text{-}H}$
	19280.4	19279.4	-	$CstR_2^{RS\text{-}SR'}$
	19302.4	19300.6	21.2	$CstR_2^{RS\text{-}SR'}$ + Na
	19312.4	19311.6	32.2	$CstR_2^{RS\text{-}S\text{-}SR'}$
	19324.4	19322.4	43	$CstR_2^{RS\text{-}SR'}$ + 2 Na

Table S3: Summary of deconvoluted CsoR masses observed by LC-ESI-MS. All mass shifts are relative to $CsoR^{RS\text{-}H}$ or $CsoR_2^{(RS\text{-}SR')}$ as indicated by (-).

Modifier	M_r Expected	M_r Observed	Mass Shift	Assignment
None	11036.6	11034.9	-	$CsoR^{RS\text{-}H}$
	11058.6	11057.0	22.1	$CsoR^{RS\text{-}H}$ + Na
SeO_3^{2-}	11036.6	11035.4	-	$CsoR^{RS\text{-}H}$
	11058.6	11057.5	22.1	$CsoR^{RS\text{-}H}$ + Na
TeO_3^{2-}	11036.6	11033.2	-	$CsoR^{RS\text{-}H}$
	21069.2	22065.4	-	$CsoR^{RS\text{-}SR'}$
	21196.8	22192.2	126.8	$CsoR_2^{RS\text{-}Te\text{-}SR'}$
	21324.4	22318.1	252.7	$CsoR_2^{(RS\text{-}Te\text{-}SR')2}$

Table S4: Summary of deconvoluted CstR cysteine mutant masses observed by LC-ESI-MS. All mass shifts are relative to $CstR^{RS\text{-}H}$ or $CstR_2^{RS\text{-}SR'}$ as indicated by (-).*

Protein	Modifier	M_r Expected	M_r Observed	Mass Shift	Assignment
C31A	None	9609.1	9607.2	-	$CstR^{RS\text{-}H}$
	MMTS	9656.2	9653.3	46.1	$CstR^{RS\text{-}SCH3}$
	SO_3^{2-}	9609.1	9606.5	-	$CstR^{RS\text{-}H}$
		9631.1	9627.9	21.4	$CstR^{RS\text{-}H}$ + Na
		9653.1	9648.6	42.1	$CstR^{RS\text{-}H}$ + 2 Na
	SeO_3^{2-}	9609.1	9606.0	-	$CstR^{RS\text{-}H}$
		9625.1	9622.3	16.3	$CstR^{RS\text{-}H}$ + O
		19216.2	19211.6	-	$CstR_2^{RS\text{-}SR'}$
		19295.2	19290.2	78.6	$CstR_2^{RS\text{-}Se\text{-}SR'}$
		19327.2	19326.4	114.8	$CstR_2^{RS\text{-}Se\text{-}SR'}$ + 2 O
	$S_4O_6^{2-}$	9609.1	9606.2	-	$CstR^{RS\text{-}H}$
		19216.2	19211.5	-	$CstR_2^{RS\text{-}SR'}$
		19232.2	19227.5	16.0	$CstR_2^{RS\text{-}SR'}$ + O
		19238.2	19232.6	21.1	$CstR_2^{RS\text{-}SR'}$ + 2 Na
		19260.2	19254.8	43.3	$CstR_2^{RS\text{-}SR'}$ + 2 Na
C60A	None	9609.1	9607.0	-	$CstR^{RS\text{-}H}$
	MMTS	9656.2	9653.5	46.5	$CstR^{RS\text{-}SCH3}$
	SO_3^{2-}	9609.1	9607.3	-	$CstR^{RS\text{-}H}$
		9631.1	9628.3	21.0	$CstR^{RS\text{-}H}$ + Na
		9689.2	9687.4	80.1	$CstR^{RS\text{-}SO3}$
		9711.2	9708.3	101.0	$CstR^{RS\text{-}SO3}$ + Na
	SeO_3^{2-}	9609.1	9606	-	$CstR^{RS\text{-}H}$
		9625.1	9622.5	16.5	$CstR^{RS\text{-}H}$ + O
		9641.1	9638.3	32.3	$CstR^{RS\text{-}H}$ + 2O
		9688.1	9684.5	78.5	$CstR^{RS\text{-}H}$ + Se
		9720.1	9717.7	111.7	$CstR^{RS\text{-}SeO2}$
		9736.1	**9738.8**	**132.8**	**$CstR^{RS\text{-}SeO3}$**
		19216.2	19211.6	-	$CstR_2^{RS\text{-}SR'}$
		19248.2	19245.4	33.8	$CstR_2^{RS\text{-}SR'}$ + 2 O
		19295.2	19290.3	78.7	$CstR_2^{RS\text{-}Se\text{-}SR'}$
		19327.2	19323.3	111.7	$CstR_2^{RS\text{-}Se\text{-}SR'}$ + 2 O
	$S_4O_6^{2-}$	9609.1	-	-	$CstR^{RS\text{-}H}$
		9721.1	9718.1	112.1	$CstR^{RS\text{-}S2O3}$
		9753.1	9750.7	144.7	$CstR^{RS\text{-}S3O3}$
C31/60A	None	9577.0	9575.3	-	No Thiol

*Major species observable by ESI-MS deconvoluted from the data shown in Fig. S4 are highlighted in *red*. The expected RS-SeO_3^{2-} adduct on Cys31 in C60A CstR is highlighted in bold font.